ELSEVIER

Chemical Geology 172 (2001) 277–290

CHEMICAL GEOLOGY
INCLUDING
ISOTOPE GEOSCIENCE

www.elsevier.com/locate/chemgeo

Obtaining geologically meaningful ^{40}Ar–^{39}Ar ages from altered biotite

H.J. Roberts [a,*], S.P. Kelley [a], P.S. Dahl [b]

[a] *Department of Earth Sciences, The Open University, Walton Hall, Milton Keynes MK7 6AA, UK*
[b] *Department of Geology, Kent State University, Kent, OH, USA*

Received 8 June 1999; accepted 17 March 2000

Abstract

Biotite is the most used ^{40}Ar–^{39}Ar geochronometer yet two significant problems arise from Ar–Ar step-heating. Dating altered biotite can be problematic, producing disturbed age spectra that reflect ^{39}Ar recoil. However, unaltered biotite can yield disturbed ages with apparently meaningful plateau ages as a result of mineral breakdown during stepped heating. Obtaining meaningful ages from such spectra is very difficult. Because alteration of biotite is common and widespread in nature, and because many biotites affected by alteration are nonetheless unique geologically and/or representative of key localities, the capability to obtain reliable ages from altered material is extremely important. In this study, the effects of alteration progress on biotite age spectra were tested using both IR laser step-heating and UV laser microprobe ^{40}Ar–^{39}Ar dating techniques. Our aims were to extract geologically meaningful ages from altered biotite and to identify cases where the ages had been influenced by alteration.

Three variably altered biotites from the Precambrian metamorphic terrain of southwestern Montana were selected for argon isotopic analysis. Sample A is an unaltered rock containing pristine biotite, sample B is a highly altered rock with chlorite and prehnite interlayers within biotite, and sample C contains biotite with only incipient alteration. For each sample, the biotite ages obtained with IR and UV laser techniques were compared and the validity of the apparent ages was assessed.

IR step-heating analysis of biotite from sample A yielded a well-defined plateau of 1776 ± 6 Ma. UV laser microprobe analysis of the same biotite yielded a concordant weighted mean age of 1771 ± 8 Ma, based upon 65 spot analyses of eight grains that ranged in age from 1819 ± 54 to 1722 ± 62 Ma. In contrast, IR step-heating of biotite from sample B resulted in disturbed spectra, with two separate fragments yielding total gas ages of 1505 ± 12 and 1540 ± 16 Ma, whereas UV laser microprobe analysis yielded 14 spot ages ranging from 1806 ± 72 to 1565 ± 78 Ma. UV laser analysis of sample C produced apparent ages ranging from 1772 ± 52 to 1359 ± 200 Ma.

Detailed analysis of age variations occurring perpendicular to (001) cleavage planes of biotite in sample B was accomplished by depth profiling using the UV laser microprobe. Depth profiling of single grains revealed considerable age variation among the biotite layers, with profiles 1 and 2 yielding apparent ages ranging from 1730 ± 226 to 1511 ± 186 Ma,

* Corresponding author.
E-mail address: hazel@rockbox.freeserve.co.uk (H.J. Roberts).

PII: S0009-2541(00)00255-2

and from 1741 ± 290 to 956 ± 230 Ma, respectively. In both samples B and C, younger apparent ages correspond to higher $^{36}Ar/^{39}Ar$ ratios. The youngest ages, therefore, are believed to have derived from altered layers, whereas the oldest ages are related to layers with relatively little or no alteration.

In summary, incremental step-heating of altered biotite single grains yields $^{40}Ar–^{39}Ar$ age spectra that are compromised by recoil and variable release patterns. However, extraction of small samples via the UV laser microprobe provides a simpler pattern of apparent ages, all younger than the "true" cooling age yet inversely correlated with atmospheric argon. This result suggests that true biotite ages can be recovered from areas of pristine material if they are sufficiently large to be ablated by the UV laser.

Keywords: $^{40}Ar–^{39}Ar$ geochronology; Alteration; Biotite; SW Montana; Precambrian

1. Introduction

Biotite is the mineral most commonly dated by K–Ar and $^{40}Ar–^{39}Ar$ geochronology. However, secondary alteration of biotite to phases such as chlorite is a common and widespread occurrence in nature and has long been known to lead to a lowering of biotite ages (Mitchell and Taka, 1984; Adams and Kelley, 1998). Although biotite ages disturbed by later heating can yield plateaux, alteration and weathering of grains almost always correlates with $^{40}Ar–^{39}Ar$ age spectra that are seriously disturbed. It is desirable to identify apparent ages that are adversely influenced by alteration and to obtain meaningful biotite ages from all rocks regardless of condition because many rocks are geologically unique and/or representative of key localities. However, producing geologically meaningful ages from highly altered biotite using incremental step-heating is difficult. Even those biotites which appear pristine in thin section can yield variable plateaux and unexpected apparent ages (e.g., Lo and Onstott, 1989; Onstott et al., 1991; Ruffet et al., 1991). Indeed, it is likely that the vast majority of natural biotites are altered to some extent. Therefore, overcoming the effects of secondary alteration on biotite age is a problem of universal importance in geochronology.

This study reports on the effects of chlorite and prehnite alteration on apparent biotite ages produced with both IR step-heating and UV laser-microprobe $^{40}Ar–^{39}Ar$ dating techniques. The results are suggestive of a useful new strategy for discriminating between meaningless "dates" in highly altered biotites and geologically meaningful ages.

2. Sample selection and experimental methods

The rocks selected for analysis in this study are high-grade gneisses from the Ruby Range, a Precambrian terrain in southwestern Montana, USA. The tectonometamorphic setting of this terrain is summarised elsewhere (e.g., Dahl et al., 1999; Mogk and Henry, 1988; Karasevich et al., 1981; Garihan, 1979; Dahl, 1979), and is not repeated here. Previous geochronology of Ruby Range phlogopites, biotites, and hornblendes has yielded $^{40}Ar–^{39}Ar$ (near-)plateau and total gas ages of ~1700 Ma (e.g., Brady et al., 1991). However, as the mica spectra were disturbed, the ~1700 Ma can be interpreted as only a minimum cooling age. In a subsequent study, Kovaric et al. (1996) produced plateau ages of ~1720 Ma for two Ruby Range phlogopites and a hornblende, using laser single-crystal fusion and furnace step-heating techniques. Extensive $^{40}Ar–^{39}Ar$ UV laser dating of biotite from across the Ruby Range by Roberts (1999) yielded biotite ages between 1780 and 1740 Ma.

Three gneisses are featured in this study: sample A, collected from the west side of the Ruby Range (Fig. 1), is a fresh, unweathered rock composed of biotite, quartz, plagioclase, garnet, and minor ilmenite. In thin section the biotite has homogeneous brown pleochroism and, at higher magnification, lacks evidence of secondary intergrowth or replacement by chlorite (Fig. 2). Sample B, collected ~10 km to the southeast of sample A (Fig. 1), is a visibly altered rock containing hornblende, biotite, sericite, quartz, plagioclase, garnet, prehnite, chlorite, and minor apatite. In contrast to sample A, the majority

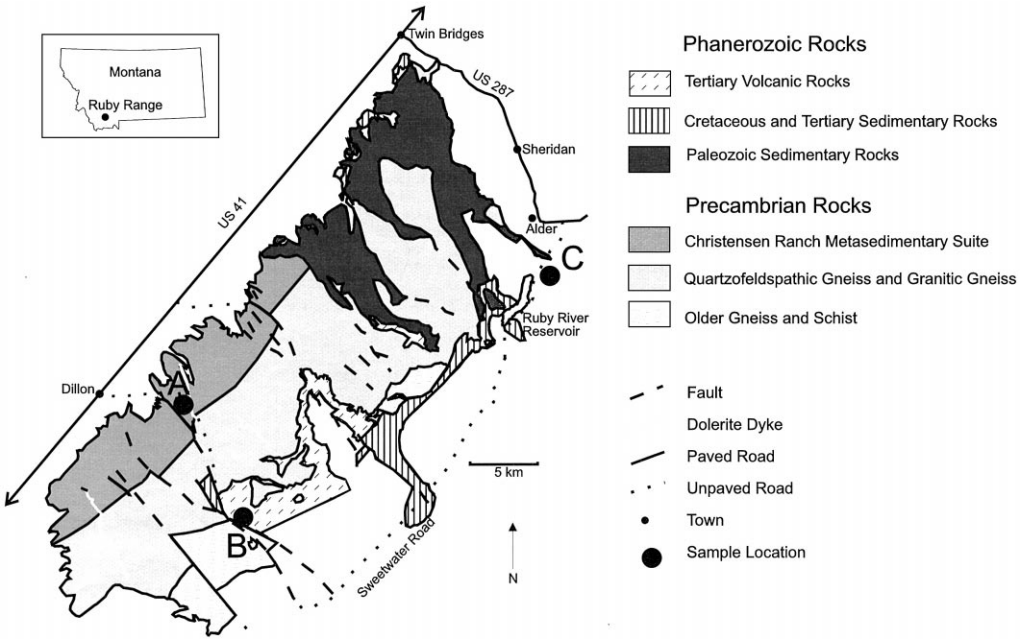

Fig. 1. Map of Ruby Range showing simplified geology and sample locations (modified from Karasevich et al., 1981).

of biotite grains in sample B appear in thin section as highly altered to chlorite and prehnite along the cleavage, and the plagioclase is heavily altered to sericite (Fig. 3). This rock is believed to have under-

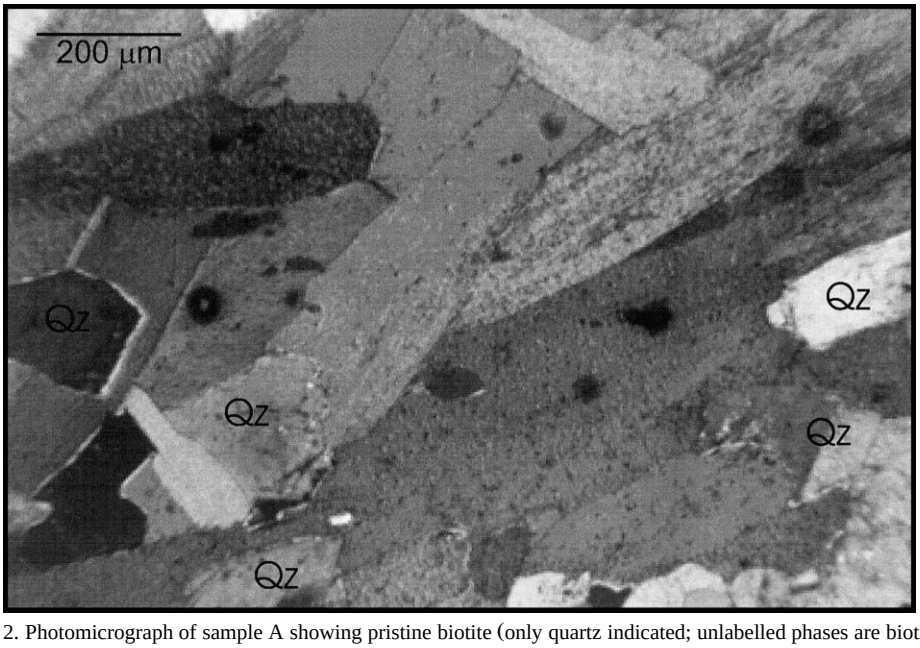

Fig. 2. Photomicrograph of sample A showing pristine biotite (only quartz indicated; unlabelled phases are biotite).

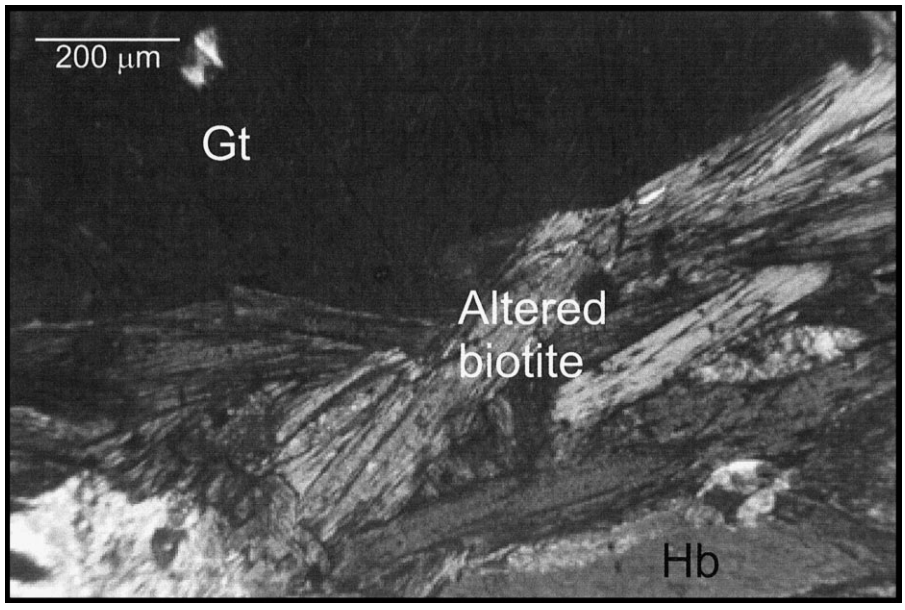

Fig. 3. Photomicrograph of sample B showing highly altered biotite.

gone calcium metasomatism due to its proximity to dolomite that has been hydrothermally altered to talc (Roberts, 1999). Average electron microprobe analyses of biotite, prehnite, and chlorite in rocks A and B are presented in Table 1.

The rocks were crushed, separated using heavy liquid, and single biotite crystals were picked by hand for subsequent irradiation and isotopic analysis. Six or seven large (millimeter scale), well-formed crystals of biotite were selected from each separate. The grains were irradiated in the McMaster reactor, Canada, for 28 h. The samples were Cd-shielded though Cl-derived ^{38}Ar was clearly still present. Analysis of five standards (Hb3gr standard with an assumed age of 1072 Ma) and calculation of the neutron flux within the reactor gave *J*-values between 0.013175 and 0.013187 $\pm$ 0.5%

Both samples underwent ^{40}Ar–^{39}Ar IR laser step-heating and UV laser microprobe analysis. The laser microprobe analyses were undertaken first and fragments of the same grains were subsequently used for the step-heating experiments.

The IR step-heating was carried out using a *Spectron Laser Systems SL902* CW Nd/YAG as the laser source, producing a continuous IR beam with a wavelength of 1064 nm. The beam, which has an output of approximately 15 W TEM_{00} and 45 W multimode (maximum), is directed into a customised

Table 1
Electron microprobe analysis of biotite from samples A–C, and of interlayer alteration minerals in sample B

Sample	SiO_2	TiO_2	Al_2O_3	MgO	CaO	MnO	FeO	Na_2O	K_2O	Total
A biotite	33.88	3.69	18.39	7.26	0.02	0.02	21.98	0.24	9.21	94.69
B biotite	33.33	3.14	14.80	11.49	0.47	0.09	22.62	0.10	5.07	91.11
B chlorite	27.84	0.66	18.14	13.43	0.11	0.19	27.08	0.02	0.64	88.10
B prehnite	42.56	0.08	23.00	0.02	27.10	0.00	1.39	0.06	0.01	94.23
C biotite	37.51	3.09	17.20	15.74	0.04	0.00	11.78	0.61	7.84	93.80

Leica Metallux 3 microscope using high reflectance, oxide coated mirrors. Focusing of the beam at the sample surface via the objective lens enabled a spot size of between 25 and 100 μm. The sample was observed using a CCD camera, coaxial with the laser beam. The grain was gently and evenly heated using a defocused laser beam over a number of steps, increasing the beam intensity with each step.

Due to the high concentrations of argon accumulated within Precambrian biotite, only small fragments of the grains analysed by UV laser microprobe were used for the IR laser step-heating experiment. Heating began with steps that caused little visible alteration to the grain. For sample A, the experiment was stopped when the fragment surface began to melt, indicated by the formation of bubbles, and the data were processed at this point. This was a large fragment that contained a considerable volume of gas and would have taken several days to analyse until all the gas was released. However, because the data showed that a plateau had already been reached, the experiment was not continued beyond the 14 steps for which data is presented in Table 1. Since the biotite fragments from sample B were smaller than those from sample A and contained less gas, the experiment on sample B was continued until the fragments were completely melted and little gas was released upon additional heating. Two fragments (1 and 2) of sample B biotite were analysed. Fragments 1 and 2 underwent 13 and 19 incremental-heating steps, respectively.

The UV laser microprobe analysis was carried out using a *Spectron Laser Systems SL401* as the source of UV radiation for sample ablation. At its source the laser has a wavelength of 1064 nm (IR). This frequency is doubled by the first KD*P crystal to 532 nm and doubled again by the second crystal to a resultant wavelength of 266 nm (UV). The wavelengths are separated using a *Pellin Brocca* prism. Typical UV laser pulses have energies of ~1 mJ/pulse, for a pulse length of 10 ns and repetition rate of 10 Hz. The beam is directed into a customised *Leica DM* microscope by high-reflectance oxide-coated mirrors. Inside the microscope the beam is redirected through a UV-refracting objective lens and focused to a spot size of ~10 μm at the sample surface. The sample is observed using a CCD camera, coaxial with the laser beam.

A computer-controlled XY stage was used to move the sample beneath the laser beam. Stage movement can be programmed to cover the area of interest and can be activated when the laser is switched on. These capabilities give the analyst precise control over the area to be ablated. For the majority of analyses a 50 μm square was ablated. The laser beam was rastered over the same area seven to nine times within the 10-min analysis time.

Detailed age variation across the cleavage planes of single biotite grains (sample B) was characterised by repeated depth-profiling of basal sections. Each analysis consisted of a 150 μm square ablated once only within the 10-min analysis time. Successive analyses were performed over the previously ablated square. Each ablation step removed only a thin layer of material. Although ^{39}Ar release has been used to calculate pit depth in K-feldspar experiments (Arnaud and Kelley, 1997), it is impossible to back-calculate the exact amount of material removed with each ablation step in biotite from sample B, using the amount of ^{39}Ar released alone. This is because alteration along the cleavage can result in potassium-depleted material being ablated during the depth profile. However, the maximum ^{39}Ar released, for a given analysis, yields an estimate of ~1 μm depth of ablation with each analysis.

The gases released were cleaned using two *SAES AP 10* getters (one at 400°C and one at room temperature). Each sample run was 10 min and the gases accumulated were equilibrated into the mass spectrometer via computer controlled *VAT* valves operated by compressed air. The extracted argon was measured in a *MAP 215-50* noble gas mass spectrometer using a *Balzers 219* electron multiplier detector. Argon isotope peaks between 35 and 41 were scanned 10 times and the amounts extrapolated back to the inlet time. Blanks were measured after every two samples and an overall mean for a day's blanks were used to correct the sample analyses.

3. Results

3.1. IR step-heating

Incremental-release step-heating of biotite in sample A yielded a well-defined plateau corresponding

to an age of 1776 ± 6 Ma (Fig. 4A, Table 2). In fact, only 5–10% of the total gas within the fragment was released during the experiment, which represents only the very beginning of the total spectrum. Clearly there is little spectral disruption, as would be expected from a pristine grain.

In contrast, spectra for the two biotite fragments from sample B both show argon loss at low temperature steps, indicating the release of argon from weakly bonded sites (Fig. 4B and C). Both reach noisy plateaux between 2134 ± 428 and 1760 ± 20 Ma. Since K–Ar biotite ages have been used routinely to date Precambrian terrains worldwide, it is instructive to see how such slight alteration affects K–Ar results. Total gas ages for biotite fragments 1 and 2 of sample B are 1505 ± 12 and 1540 ± 16 Ma, respectively (Fig. 4B and C, Table 2).

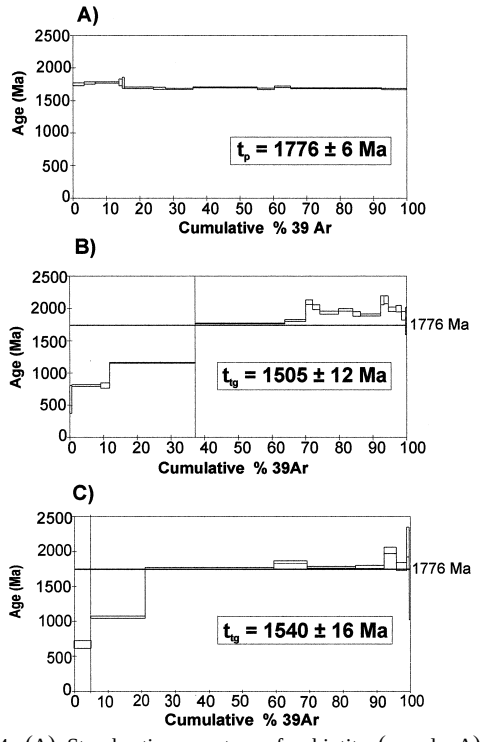

Fig. 4. (A) Step-heating spectrum for biotite (sample A). (B) Step-heating spectrum for biotite (sample B, fragment 1). (C) Step-heating spectrum for biotite (sample B, fragment 2).

3.2. UV microprobe analysis

One of the difficulties in working with the UV data is the small gas volumes produced. In any study of this sort, the analyst walks a fine line between ablating sufficient material to gain a high enough signal-to-noise ratio and removing small amounts of material to pick up the increasingly small-scale oscillations present in the mineral itself. The difficulty is highlighted by the large analytical errors presented by the spot analyses, especially in the altered grains.

A total of 65 spots were analysed in eight grains of biotite from sample A. Spot ages ranged from 1819 ± 54 to 1715 ± 34 Ma, corresponding to a weighted mean of 1771 ± 8 Ma (Table 3). A total of 14 analyses (eight from grain 1 alone) were carried out on (relatively altered) biotite from sample B. Spot ages for grain 1 ranged from 1697 ± 56 to 1565 ± 78 Ma, whereas the other six ages ranged from 1806 ± 72 to 1740 ± 96 Ma (Table 3).

Two age–depth profiles were produced for sample B (grain 1), as shown in Fig. 5. Because of the small amount of material ablated in each analysis of the depth profile, the errors associated with these dates are relatively high in comparison to the spots in the same sample. However, both profiles reveal significant age variation with depth. Apparent ages of biotite layers range from 1730 ± 226 to 1511 ± 186 Ma (profile 1) and from 1741 ± 290 to 956 ± 230 Ma (profile 2), as indicated in Fig. 5a–b and Table 4. These two profiles demonstrate how chlorite variations within individual grains can produce variable profiles. Fig. 5a shows little variation, whereas Fig. 5b shows considerable variation.

In order to investigate potential relationships among apparent age, biotite composition, and/or atmospheric content, the ratios of $^{38}Ar/^{39}Ar$, $^{37}Ar/^{39}Ar$ and $^{36}Ar/^{39}Ar$ were calculated for all the data from both samples (Tables 2–4). The $^{36}Ar/^{39}Ar$ ratios were plotted against $^{40}Ar/^{39}Ar$ age as shown in Fig. 6a, b, and c. Fig. 6a–c consistently show strong correlation between the $^{36}Ar/^{39}Ar$ ratio and apparent age, with the younger apparent ages corresponding to the higher $^{36}Ar/^{39}Ar$ ratios. The $^{36}Ar/^{39}Ar$ ratios for altered sample B range from −0.006 to 0.072 (Table 4), whereas in unaltered sample A the ratios only range from −0.008 to 0.023 (Table 3); similarly, samples B and A exhibit maximum atmospheric argon of 25% and 5%, respectively. These trends

Table 2
IR laser step-heating analysis for samples A and B

Sample	Step	$^{40}Ar/^{39}Ar$	$^{38}Ar/^{39}Ar$	$^{37}Ar/^{39}Ar$	$^{36}Ar/^{39}Ar$	% ^{39}Ar	$^{40}Ar^{*}/^{39}Ar$	Age (Ma)	$\pm 1\sigma$
A	1	127.87	0.02	0.00	0.013	3.57	124.02	1748	22
	2	126.04	0.01	−0.03	0.000	7.10	126.12	1767	16
	3	127.30	0.01	−0.01	0.001	14.73	126.98	1775	11
	4	127.70	0.00	−0.02	0.001	15.79	127.45	1779	50
	5	131.42	0.03	−0.14	0.016	16.43	126.79	1773	82
	6	129.82	0.01	0.01	0.008	24.98	127.58	1780	12
	7	127.81	0.02	0.00	0.004	28.58	126.68	1772	16
	8	128.07	0.01	0.01	0.008	36.73	125.86	1765	9
	9	129.02	0.01	0.00	0.002	55.74	128.44	1788	7
	10	126.69	0.01	0.01	0.002	60.81	126.00	1766	12
	11	131.06	0.02	0.01	0.005	65.66	129.67	1798	13
	12	127.39	0.01	0.00	0.001	80.03	127.03	1775	7
	13	127.08	0.02	0.00	0.001	92.59	126.89	1774	7
	14	126.35	0.01	0.00	0.002	100.00	125.66	1763	9
B									
Fragment 1	1	13.09	0.47	0.50	−0.677	−0.12	213.13	2412	1255
	2	68.16	0.04	0.02	0.116	4.94	34.02	668	56
	3	20.00	0.31	−3.95	−1.946	4.89	595.11	nd	
	4	−52.98	−0.17	−4.24	0.556	4.85	−217.30	nd	
	5	70.08	0.02	0.00	0.032	21.05	60.53	1058	14
	6	132.88	0.02	0.00	0.025	59.39	125.43	1760	10
	7	139.57	0.02	0.02	0.015	69.27	135.05	1844	19
	8	130.50	0.02	0.00	0.013	83.70	126.79	1772	14
	9	129.77	0.01	0.03	0.008	92.21	127.32	1777	22
	10	162.39	−0.02	−0.01	0.022	95.93	155.99	2015	45
	11	142.85	0.05	0.10	0.050	98.92	127.95	1782	58
	12	175.82	−0.01	−0.12	0.014	99.66	171.80	2134	214
	13	116.85	0.17	1.21	0.449	100.00	−15.87	nd	
Fragment 2	1	123.05	0.05	−0.10	0.318	0.57	29.17	587	216
	2	61.10	0.03	0.00	0.063	9.19	42.50	802	13
	3	56.64	0.02	0.02	0.048	11.85	42.48	802	42
	4	74.33	0.02	0.00	0.021	37.24	68.24	1157	6
	5	120.16	0.41	3.03	1.037	37.28		nd	
	6	129.14	0.02	0.00	0.010	63.85	126.09	1766	7
	7	135.26	0.02	0.01	0.013	70.06	131.52	1814	14
	8	165.90	0.01	0.01	−0.002	72.16	166.53	2095	37
	9	154.51	0.00	−0.01	−0.007	74.27	156.50	2019	38
	10	143.67	0.01	0.00	−0.007	79.79	145.74	1933	25
	11	153.65	0.03	−0.02	0.009	84.05	150.91	1975	19
	12	144.19	0.01	0.05	0.002	86.30	143.49	1915	35
	13	140.25	0.01	0.02	−0.004	92.33	141.43	1898	16
	14	165.26	−0.01	0.06	−0.019	93.35	170.79	2127	72
	15	169.73	0.01	0.01	−0.008	94.56	172.01	2135	61
	16	154.32	0.02	0.03	0.006	96.92	152.44	1987	33
	17	147.18	−0.01	0.01	−0.022	98.46	153.67	1997	50
	18	145.18	0.03	0.04	0.017	99.63	140.13	1887	68
	19	126.77	0.15	−0.05	−0.012	100.00	130.35	1803	210

indicate that apparent age is inversely correlated with degree of alteration in the cleavage. The $^{37}Ar/^{39}Ar$ and $^{38}Ar/^{39}Ar$ ratios fail to exhibit similar correlation, which indicates that the alteration is not intro-

Table 3
UV laser microprobe analysis for samples A–C. UV laser $^{40}Ar/^{39}Ar$ analyses of unaltered biotite yielded many ^{36}Ar peak measurements on the mass spectrometer that were less than the blank value (which was in turn dominated by the mass spectrometer background value). However, the variation of blanks was greater than the amounts of ^{36}Ar measured in samples and thus the pooled sample ^{36}Ar peak is within errors of a pooled blank. In altered samples, ^{36}Ar peak measurements were more often obscured but all data tables reflect the very small amount of ^{36}Ar measured in the number of apparently negative $^{36}Ar/^{39}Ar$ ratios. All negative values are, however, within error of zero

Sample	Grain	$^{40}Ar/^{39}Ar$	$^{38}Ar/^{39}Ar$	$^{37}Ar/^{39}Ar$	$^{36}Ar/^{39}Ar$	^{39}Ar (cm^3) $\times 10^{-11}$	$^{40}Ar^*/^{39}Ar$	Age (Ma)	$\pm 1\sigma$
A	1	124.41	0.01	−0.01	−0.001	2.68	124.77	1755	32
		120.37	0.01	0.00	−0.003	2.83	121.18	1722	31
		123.34	0.01	0.00	−0.007	2.84	125.55	1762	28
		123.67	0.01	0.00	0.005	3.12	122.27	1732	25
		124.19	0.01	−0.01	−0.005	3.08	125.80	1764	26
		128.57	0.01	0.00	0.000	3.08	128.45	1788	28
		127.74	0.01	0.00	−0.003	2.99	128.51	1788	26
		125.10	0.01	0.00	0.005	3.12	123.70	1745	31
		125.25	0.01	0.01	−0.004	3.03	126.44	1770	29
		123.50	0.01	0.01	−0.003	3.06	124.24	1750	30
		121.32	0.01	−0.01	−0.002	3.14	122.04	1730	28
		123.89	0.01	0.00	−0.001	3.09	124.19	1750	27
	2	120.66	0.01	−0.01	−0.002	2.6	121.37	1724	34
		122.81	0.02	−0.01	−0.010	2.43	125.76	1764	29
		122.66	0.01	−0.01	−0.001	3.25	122.82	1737	26
		126.52	0.01	−0.01	−0.001	3.22	126.68	1772	24
		128.63	0.01	−0.01	−0.002	3.36	129.19	1794	28
		126.42	0.01	−0.02	−0.008	3.21	128.66	1790	26
		126.12	0.01	0.00	0.007	3.63	124.07	1749	25
		128.47	0.02	−0.01	−0.006	3.29	130.25	1804	27
		126.60	0.01	−0.01	−0.002	3.43	127.14	1776	26
		125.42	0.01	−0.02	−0.005	3.27	126.80	1773	27
		125.68	0.01	0.00	−0.002	3.23	126.25	1768	31
		128.06	0.01	0.00	−0.001	3.36	128.22	1786	27
		126.41	0.01	0.00	−0.003	3.15	127.42	1779	23
		128.37	0.01	−0.02	0.001	3.47	128.14	1785	31
		124.58	0.01	0.00	−0.003	3.45	125.51	1762	25
		123.74	0.01	−0.01	0.001	3.61	123.51	1744	28
		128.53	0.01	−0.01	−0.003	3.38	129.47	1797	25
		128.34	0.01	−0.02	0.001	3.28	128.09	1785	25
		127.83	0.01	−0.01	−0.005	3.32	129.20	1794	24
		127.49	0.01	−0.02	−0.002	3.46	128.02	1784	22
		122.22	0.01	0.00	−0.006	3.52	123.88	1747	26
		126.07	0.01	−0.01	−0.004	3.7	127.29	1778	23
		125.64	0.01	−0.01	−0.003	3.65	126.51	1771	23
		126.10	0.01	−0.01	−0.006	3.07	128.00	1784	28
		125.45	0.01	−0.01	0.006	3.35	123.63	1745	25
		127.82	0.01	−0.01	−0.002	3.35	128.38	1787	22
		122.26	0.01	0.00	−0.008	3.6	124.62	1754	24
		123.09	0.01	0.00	0.000	3.64	123.24	1741	22
		127.27	0.01	0.00	−0.002	3.56	127.79	1782	26
		128.45	0.01	0.00	0.002	3.79	127.88	1783	25
		124.83	0.01	−0.01	−0.002	3.87	125.31	1760	21
		127.43	0.01	−0.01	−0.005	3.77	128.98	1793	23
		124.44	0.01	−0.01	0.000	3.9	124.58	1753	25
		123.70	0.01	−0.01	0.000	3.87	123.84	1747	27
		128.24	0.01	−0.01	−0.004	3.69	129.47	1797	22
	3	122.71	0.01	−0.01	−0.005	4.18	124.11	1749	26

Table 3 (*continued*)

Sample	Grain	$^{40}Ar/^{39}Ar$	$^{38}Ar/^{39}Ar$	$^{37}Ar/^{39}Ar$	$^{36}Ar/^{39}Ar$	^{39}Ar (cm^3) $\times 10^{-11}$	$^{40}Ar^*/^{39}Ar$	Age (Ma)	$\pm 1\sigma$
		123.26	0.02	−0.01	−0.001	5.16	123.56	1744	23
		123.59	0.01	0.00	−0.002	5.38	124.13	1749	18
		124.89	0.01	0.00	−0.001	5.56	125.17	1759	18
		130.63	0.01	−0.01	−0.005	5.09	131.99	1819	27
		124.77	0.01	0.00	−0.004	5.74	125.97	1766	16
	4	128.39	0.01	0.00	0.005	5.67	127.03	1775	32
		125.03	0.01	0.00	−0.002	5.98	125.74	1764	17
	5	123.42	0.01	−0.01	−0.008	5.01	125.86	1765	18
	6	125.14	0.01	−0.01	0.003	2.35	124.12	1749	42
		132.71	0.01	0.00	0.023	3.13	126.01	1766	38
	7	125.70	0.01	0.00	0.001	5.82	125.52	1762	26
	8	122.91	0.01	0.01	0.002	5.23	122.46	1734	23
		120.57	0.01	0.01	0.001	6.61	120.41	1715	17
		123.28	0.02	0.00	−0.003	7.14	124.25	1750	13
		129.39	0.01	−0.01	0.000	6.45	129.44	1797	37
		123.35	0.01	0.00	0.000	6.55	123.39	1743	21
		126.59	0.01	−0.01	0.002	6.18	125.99	1766	27
B	1	112.08	0.02	0.03	0.020	2.17	106.15	1578	42
		110.33	0.01	0.02	0.019	2.57	104.81	1565	39
		111.94	0.01	0.01	−0.002	2.6	112.62	1641	34
		111.93	0.00	0.02	0.006	2.83	110.21	1618	35
		113.21	0.01	0.00	0.016	3.08	108.60	1602	26
		112.61	0.02	−0.01	0.015	3.23	108.22	1599	29
		118.71	0.01	0.00	0.001	4.51	118.52	1697	28
		114.66	0.02	0.01	0.005	4.95	113.14	1646	26
	2	130.10	0.02	0.01	0.023	3.23	123.18	1740	48
		125.49	0.02	0.00	0.004	4.1	124.26	1749	39
		126.83	0.01	0.00	−0.003	3.86	127.59	1779	40
		123.37	0.01	0.01	−0.006	4.07	125.07	1757	38
	3	126.78	0.01	0.01	−0.006	5	128.43	1787	40
	4	130.29	0.01	−0.01	−0.001	4.31	130.66	1806	39
C	1	122.03	0.01	0.01	0.005	2.14	120.63	1721	46
		122.14	0.02	0.01	0.016	2.01	117.35	1690	62
		112.32	0.01	0.00	0.009	1.57	109.56	1616	63
		100.56	0.02	0.02	0.027	1.53	92.51	1442	77
		98.21	0.02	0.02	0.004	1.59	97.17	1491	64
		92.09	0.02	−0.01	0.013	1.49	88.31	1396	77
	2	126.83	0.02	0.01	0.019	1.79	121.26	1726	35
		123.69	0.01	−0.01	−0.003	2.6	124.46	1755	34
		124.62	0.01	0.00	0.006	2.53	122.78	1740	33
		125.74	0.01	0.00	0.008	2.58	123.42	1746	32
		121.55	0.02	0.01	0.008	2.51	119.17	1707	36
	3	121.58	0.01	0.00	0.013	2.87	117.63	1693	35
	4	115.11	0.03	0.53	0.033	6.8	105.34	1574	794
	5	99.24	0.03	−0.03	0.048	8.85	84.96	1359	100
	6	123.03	0.01	0.00	0.001	4.68	122.60	1739	23
	7	125.73	0.01	−0.01	−0.002	3.44	126.31	1772	26

ducing Ca or Cl into the biotite. Superficially it appears possible to set a $^{36}Ar/^{39}Ar$ "altered" criterion but the depth profiles in sample B show that the alteration is not always as easy to detect. Increases in

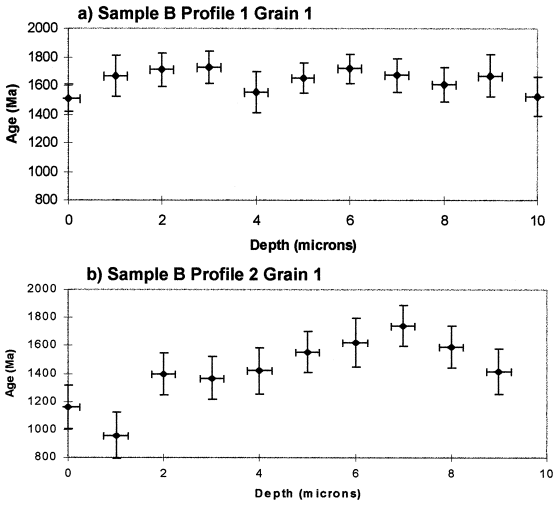

Fig. 5. (a) Apparent $^{40}Ar/^{39}Ar$ age versus approximate depth (sample B, profile 1, grain 1). (b) Apparent $^{40}Ar/^{39}Ar$ age versus approximate depth (sample B, profile 2, grain 1).

$^{36}Ar/^{39}Ar$ are often small and such a criterion would vary with each irradiation.

4. Discussion

Sample A biotite represents an ideal grain for ^{40}Ar–^{39}Ar dating, giving reproducible ages with a high level of confidence (Fig. 2a, Tables 2 and 3). In contrast, "ages" from sample B biotite vary considerably with each analysis and technique. As shown in Fig. 2b and c, sample B biotite yields disturbed spectra when step-heated using the IR laser. Thus, in the absence of other data, all that normally could be inferred for this biotite is that its true age lies between the total gas age of $\sim$1500 Ma and the plateau of 1900 Ma. However, the UV microprobe data can further refine the age of this sample, as discussed below.

UV laser microprobe dating of sample A biotite (Fig. 4a, Table 3) indicates that the age of unaltered rocks from location A and environs (Fig. 1) is 1771 $\pm$ 8 Ma. For sample B biotite, the majority of age variation is confined to grain 1; in contrast, the six ages from grains 2 to 4 define a mean of 1770 $\pm$ 40 Ma, which represents excellent agreement with sample A. This suggests that these grains were less

Table 4
UV laser microprobe depth profiles for sample B, grain 1

Sample	Profile	$^{40}Ar/^{39}Ar$	$^{38}Ar/^{39}Ar$	$^{37}Ar/^{39}Ar$	$^{36}Ar/^{39}Ar$	^{39}Ar (cm^3) $\times 10^{-12}$	$^{40}Ar^*/^{39}Ar$	Age (Ma)	$\pm 1\sigma$
B	1	120.88	0.01	0.03	0.072	7.56	99.47	1511	93
		126.49	−0.01	0.06	0.037	5.08	115.58	1669	141
		120.38	0.00	0.07	0.001	5.76	119.99	1711	119
		120.32	0.01	−0.02	−0.006	6.05	122.15	1730	113
		111.28	−0.01	0.03	0.025	5.71	103.91	1556	143
		120.83	0.02	0.00	0.024	6.00	113.82	1653	103
		116.52	0.01	0.01	−0.014	5.76	120.76	1718	102
		116.25	0.01	0.00	0.001	5.18	115.82	1672	120
		109.60	0.02	−0.03	0.001	5.18	109.17	1608	122
		115.98	0.00	−0.04	0.002	4.84	115.52	1669	147
		111.39	0.00	−0.06	0.036	5.27	100.88	1525	137
	2	78.82	0.04	0.10	0.035	5.09	68.38	1159	154
		70.58	0.03	0.17	0.059	4.55	53.06	956	165
		100.50	0.02	0.02	0.040	4.55	88.81	1398	149
		89.05	0.01	0.03	0.010	4.55	86.13	1368	154
		101.71	0.03	−0.04	0.037	3.65	90.79	1419	165
		103.83	0.04	−0.03	0.000	3.52	103.83	1555	147
		106.65	0.02	−0.08	−0.013	3.52	110.43	1620	173
		112.26	0.02	0.05	−0.037	3.61	123.32	1741	145
		107.30	0.00	−0.06	0.000	3.74	107.30	1590	149
		100.68	0.04	−0.05	0.035	3.88	90.39	1415	159

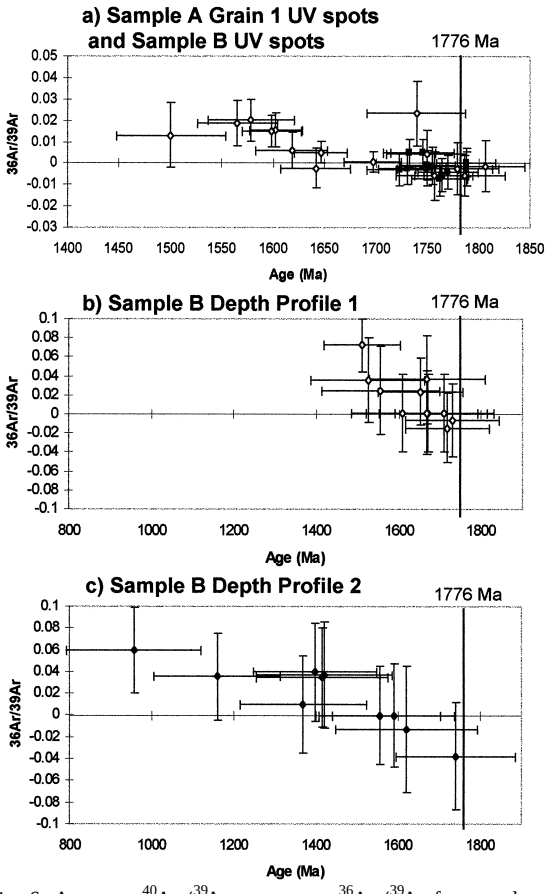

Fig. 6. Apparent $^{40}Ar/^{39}Ar$ age versus $^{36}Ar/^{39}Ar$ for samples A (grain 1 only) and B (UV spots and depth profiles).

altered than grain 1. For a rock containing both altered and unaltered biotite, such concordance suggests that a meaningful age cannot be obtained by step-heating the bulk sample but may be acquired only by rigorous exclusion of altered grains.

In sample B, alteration of biotite occurs principally along the cleavage planes, as indicated microscopically. Isotopic depth profiling of the most altered grain (grain 1) seems to have discriminated between altered and less altered areas, with different layers showing variations of several hundred million years (Fig. 3a and b, Table 4). Conceivably, the younger apparent ages revealed by this UV depth profiling might be caused by loss of ^{40}Ar (or gain in ^{39}Ar due to recoil), which ultimately affects the $^{40}Ar/^{39}Ar$ ratio. Previous work has shown that ^{39}Ar is locally recoiled during neutron irradiation (Turner and Cadogan, 1974; Onstott et al., 1995; Villa, 1997). When ^{39}Ar from the K-rich layer recoils into an adjacent K-poor layer, the ^{39}Ar abundance in the K-poor layer increases in relation to that of the ^{40}Ar. This results in a lower $^{40}Ar/^{39}Ar$ ratio, thereby giving an apparent age that is anomalously young. In theory, loss of potassium might cause age increases, but evidence from K–Ar studies shows that K loss is accompanied by greater loss of ^{40}Ar and thus results in younger apparent ages (Mitchell and Taka, 1984). Alteration tends to produce biotite interlayered with minerals such as chlorite, thereby introducing a K-poor layer. Depth profiling through such a mineral analyses K-rich biotite layers, K-poor alteration layers, or a combination of the two. Published data show that K-poor layers tend to produce lower apparent ages in agreement with the bulk K–Ar data (Mitchell and Taka, 1984).

Given that previous step-heating studies have shown age variations assigned to recoil (Lo and Onstott, 1989; Ruffet et al., 1991), it is possible that the UV laser age variations described in this study are also caused by ^{39}Ar recoil. Recoil energies of around 300 keV cause the atoms to recoil distances of around 0.08 μm across a boundary (Villa, 1997 and references therein). The depth of each ablated volume analysed in our UV laser microprobe experiments was calculated to be ~1 μm, based upon ^{39}Ar release (as described above). Given that the recoil distances are much less than each layer of biotite stripped off by the laser (~10%), it is possible to demonstrate, in a simple way, that recoil is unlikely to be important.

Onstott et al. (1995) calculated the distribution of ^{39}Ar via recoil into a semi-infinite space showing that the ^{39}Ar recoil profile approximates to an exponential with a mean depletion depth of 0.0818 μm. As pointed out by Onstott et al. (1995) this is half the full recoil penetration distance and leads to approximately 10% ^{39}Ar depletion into a semi-infinite space. Given the potassium content is 50% less in the altered zones (see discussion above) recoil back into the undepleted layer would result in final ^{39}Ar contents 5% low in the undepleted layer but 10% high in the altered zone.

The $^{40}Ar/^{39}Ar$ ratio measured for altered biotite layers in sample B ranged from 53.0 (956 Ma) to

123.3 (1741 Ma) (see Table 4). If maximum recoil had occurred then these measurements were enriched in ^{39}Ar by 10% which would cause a correspondingly reduction in $^{40}Ar/^{39}Ar$ by 10%. In other words, the $^{40}Ar/^{39}Ar$ ratios would have been 58.5 and 135.7, respectively, before recoil, indicating older actual ages of 1034 and 1854 Ma. Thus even if recoil is removed assuming maximum effect, the youngest age recorded in altered layers was only 1034 Ma, significantly below the age of 1770 Ma recorded in the unaltered sample, A. In fact, over 60% of the ages in the depth profile of sample B are significantly younger than 1770 Ma even when recoil is taken away at the maximum possible level. Therefore, although recoil may be contributing to the age variations observed for sample B biotite, it is unlikely to be an important consideration.

We have inferred that the youngest apparent ages are dominated by zones of alteration along the cleavages, whereas the oldest ages are locally preserved in unaltered or less altered biotite between the cleavages. The older ages in the depth profiles in sample B range from 1741 ± 290 Ma (2σ) to 1711 ± 238 Ma (2σ), which is concordant within (large) error to the 1770 Ma age of unaltered biotite in sample A. Thus, even in the most highly altered grains, apparent ages approximating the true age of the sample can be obtained.

It is important to note in this context that the IR step-heated biotite from sample B not only yielded low ages in the initial release but also anomalously high ages at high temperature. This effect was not seen in the UV analysis and may truly result from recoil of ^{39}Ar from sites releasing at the higher temperatures. In this case, the UV spot analysis revealed more reliable and reproducible ages than the IR step-heating, even though the step-heating was undertaken on entire single grains.

5. Application of the technique to slightly altered biotite grains

Biotite from a third metamorphic rock (sample C; see Fig. 1) was analysed to determine if biotite with only very slight visual indication of alteration would also produce younger ages with corresponding higher $^{36}Ar/^{39}Ar$ ratios. Under the petrographic microscope sample C biotite appears to represent a good candidate for ^{40}Ar–^{39}Ar dating (see Fig. 7). At high mag-

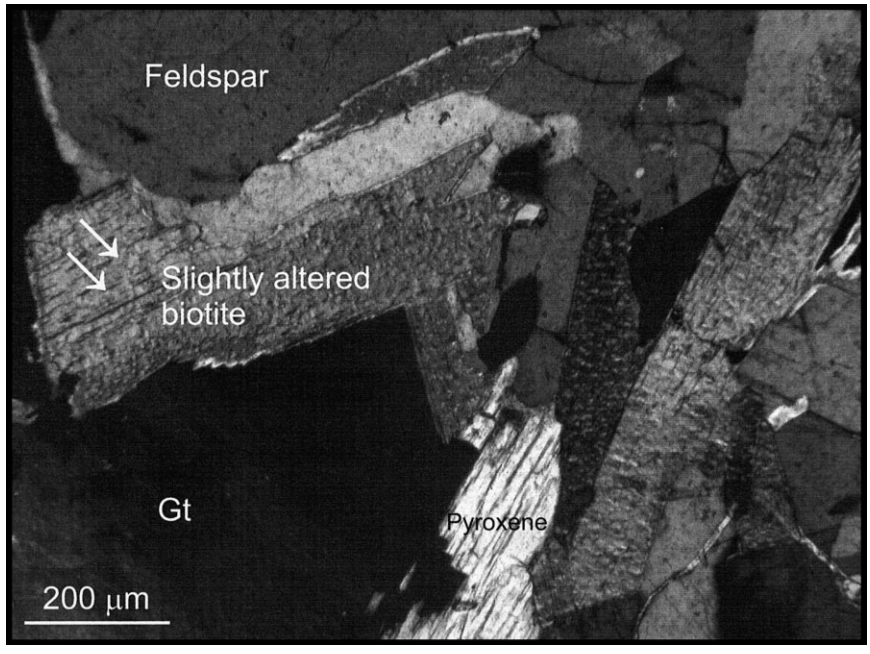

Fig. 7. Photomicrograph of sample C showing alteration of biotite.

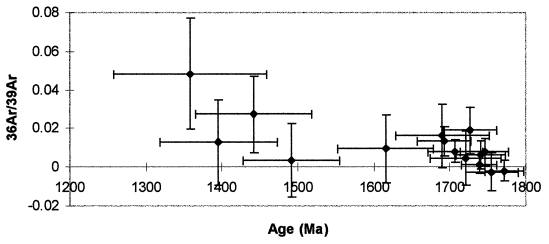

Fig. 8. Apparent $^{40}Ar/^{39}Ar$ ages versus $^{36}Ar/^{39}Ar$ ratio (sample C).

nification, however, slight green and brown mottling of the grains is revealed as patches less than 100 μm across.

These biotites were prepared and irradiated in the same way as described previously, and 50 μm squares were analysed using the UV laser microprobe. Areas without microscopic alteration within single grains gave ages ranging from 1772 ± 52 to 1721 ± 92 Ma, consistent with the biotite age obtained in sample A. In contrast, areas with evident alteration gave lower dates ranging from 1690 ± 124 to 1359 ± 200 Ma, with the low levels of argon released leading to relatively large errors (see Table 3). Thus, within a single grain an apparent difference of ~ 360 Ma was recorded from the altered to unaltered sub-grain domains. Again, examination of the $^{36}Ar/^{39}Ar$ ratio shows that ^{36}Ar abundances were higher in the analyses yielding the younger apparent ages (Fig. 8).

This experiment demonstrates that even incipiently altered biotite displays younger apparent ages with correspondingly higher $^{36}Ar/^{39}Ar$ ratios. Further, it is demonstrated that meaningful $^{40}Ar/^{39}Ar$ ages can be obtained even from an altered biotite, by careful and selective in situ analysis of argon isotopes.

6. Conclusions

1. Step-heating altered biotite grains frequently produces disturbed $^{40}Ar/^{39}Ar$ spectra that are difficult to interpret, which propagates as loss of analytical confidence in the inferred ages. The interaction of recoil phenomena and variable release from low- and high-K phases leads to anomalously low and anomalously high ages.

2. Selective UV laser microanalysis of unaltered biotite grains within an altered sample, or of unaltered domains within altered biotite grains, can produce ages that are consistent with the true age. In the case of highly altered biotites, only minimum ages close to the true age can be expected.

3. In many cases, the presence of alteration in biotite may be identified by a high $^{36}Ar/^{39}Ar$ ratio, even where thin section examination indicates very little alteration. This is only possible on very low blank UV laser analyses.

4. Even apparently pristine biotite may contain incipient alteration that will have a significant effect on apparent ages, unless selective microanalysis is undertaken. The UV laser microprobe analysis is eminently suited for this work. Moreover, the UV laser microprobe can yield good ages even for highly altered samples. This is true because the areas extracted can be tightly controlled rather than released from a bulk sample and mixed with gas from altered areas.

Acknowledgements

Thorough reviews by W. Hames and M. Villeneuve greatly improved this paper. H. Roberts was supported by an Open University grant during this research. P. Dahl gratefully acknowledges research travel support from NSF grant EAR-9614822.

References

Adams, C.J., Kelley, S., 1998. Provenance of Permian–Triassic and Ordovician metagraywacke terranes in New Zealand: evidence from $^{40}Ar/^{39}Ar$ dating of detrital micas. Geol. Soc. Am. Bull. 110, 422–432.

Arnaud, N., Kelley, S., 1997. Argon behaviour in gem-quality orthoclase from Madagascar, experiments and some consequences for $^{40}Ar/^{39}Ar$ geochronology. Geochim. Cosmochim. Acta 61, 3227–3255.

Brady, J.B., Cheney, J.T., Duvall, M.L., Green, C., Kaufman, L., Kogut, A.I., Larson, A.C., Vasquez, A., 1991. Metasomatic talc deposits in southwestern Montana: geochemical evidence for deep circulation of water-rich fluids. Geol. Soc. Am., Abstr Programs 23 (5), 30463.

Dahl, P.S., 1979. Comparative geothermometry based on major-element and oxygen isotope distributions in Precambrian metamorphic rocks form southwestern Montana. Am. Mineral. 64, 1280–1293.

Dahl, P.S., Holm, D.K., Gardner, E.T., Hubacher, F.A., Foland, K.A., 1999. New constraints on the timing of Early Proterozoic tectonism in the Black Hills (South Dakota), with implications for docking of the Wyoming province with Laurentia. Geol. Soc. Am. Bull. (in press).

Garihan, J.M., 1979. Geology and structure of the central Ruby Range, Madison County, Montana. Geol. Soc. Am. Bull. 90, 695–788.

Karasevich, L.P., Garihan, J.M., Dahl, P.S., Okuma, A.F., 1981. Summary of Precambrian metamorphic and structural history, Ruby Range, southwest Montana. Mont. Geol. Soc. 225–237.

Kovaric, D.N., Brady, J.B., Cheney, J.T., Grove, M., Jacob, L.T., King, J.T., 1996. $^{40}Ar/^{39}Ar$ evidence for reheating events affecting basement rocks in the Tobacco Root, Ruby and Highland Mountains, southwest Montana. Geol. Soc. Am., Abstr. Programs 28 (7), A-493.

Lo, C.H., Onstott, T.C., 1989. ^{39}Ar recoil artefacts in chloritized biotite. Geochim. Cosmochim. Acta 53, 2697–2711.

Mitchell, J.G., Taka, A.S., 1984. Potassium and argon loss patterns in weathered micas: Implications for detrital mineral studies, with particular reference to the Triassic palaeogeography of the British Isles. Sediment. Geol. 39, 27–52.

Mogk, D.M., Henry, D.J., 1988. Metamorphic petrology of the northern Archean Wyoming province, southwestern Montana: evidence for Archean collisional tectonics. In: Ernst, W.G. (Ed.), Metamorphism and Crustal Evolution of the Western United States. Rubey Vol. VII, pp. 362–382.

Onstott, T.C., Phillips, D., Pringle-Goodell, L., 1991. Laser microprobe measurement of chlorine and argon zonation in biotite. Chem. Geol. 90, 145–168.

Onstott, T.C., Miller, M.L., Ewing, R.C., Arnold, G.W., Walsh, D.S., 1995. Recoil refinements: implications for the $^{40}Ar/^{39}Ar$ dating technique. Geochim. Cosmochim. Acta 59, 1821–1834.

Roberts, H.J. (1999). An investigation of a polymetamorphic terrain using $^{40}Ar–^{39}Ar$ geochronology. Unpublished PhD thesis. The Open University.

Ruffet, G., Féraud, G., Amouric, M., 1991. Comparison of $^{40}Ar–^{39}Ar$ conventional and laser dating of biotites from the North Trégor Batholith. Geochim. Cosmochim. Acta 55, 1675–1688.

Turner, G., Cadogan, P.H., 1974. Possible effects of ^{39}Ar recoil in $^{40}Ar–^{39}Ar$ dating. Proc. Fifth Lunar Sci. Conf. 2, 1601–1615.

Villa, I., 1997. Direct determination of ^{39}Ar recoil distance. Geochim. Cosmochim. Acta 61, 689–691.